the plant journal

SEB Society for Experimental Biology

The Plant Journal (2017) **90,** 418–430 doi: 10.1111/tpj.13494

TECHNICAL ADVANCE

Subunit-selective proteasome activity profiling uncovers uncoupled proteasome subunit activities during bacterial infections

Johana C. Misas-Villamil[1,2], Aranka M. van der Burgh[1,†], Friederike Grosse-Holz[3], Marcel Bach-Pages[3], Judit Kovács[1,4], Farnusch Kaschani[5], Sören Schilasky[1], Asif E.K. Emon[1,‡], Mark Ruben[6], Markus Kaiser[5], Hermen S. Overkleeft[6] and Renier A.L. van der Hoorn[1,3,*]

[1]*The Plant Chemetics Laboratory, Max Planck Institute for Plant Breeding Research, Carl-von-Linné Weg 10, 50829 Cologne, Germany,*

[2]*Botanical Institute and Cluster of Excellence on Plant Sciences, University of Cologne, 50674 Cologne, Germany,*

[3]*The Plant Chemetics Laboratory, Department of Plant Sciences, University of Oxford, South Parks Lane, Oxford OX1 3RB, UK,*

[4]*Department of Plant Biology, University of Szeged, Szeged, Hungary,*

[5]*Chemical Biology, Universität Duisburg-Essen, Zentrum für Medizinische Biotechnologie, Fakultät für Biologie, Universitätsstr. 2, 45117 Essen, Germany, and*

[6]*Gorlaeus Laboratories, Institute of Chemistry and Netherlands Proteomics Centre, 2333 CC Leiden, The Netherlands*

Received 6 May 2016; accepted 9 January 2017; published online 24 January 2017.

*For correspondence (e-mail renier.vanderhoorn@plants.ox.ac.uk).

[†]Present address: Laboratory for Phytophathology, Wageningen University, Droevendaalsesteeg 1, 6708 PB, Wageningen, The Netherlands.

[‡]Present address: Bonn-Aachen International Center for IT, University of Bonn, Dahlmannstrasse 2, 53113, Bonn, Germany.

SUMMARY

The proteasome is a nuclear-cytoplasmic proteolytic complex involved in nearly all regulatory pathways in plant cells. The three different catalytic activities of the proteasome can have different functions, but tools to monitor and control these subunits selectively are not yet available in plant science. Here, we introduce subunit-selective inhibitors and dual-color fluorescent activity-based probes for studying two of the three active catalytic subunits of the plant proteasome. We validate these tools in two model plants and use this to study the proteasome during plant–microbe interactions. Our data reveal that *Nicotiana benthamiana* incorporates two different paralogs of each catalytic subunit into active proteasomes. Interestingly, both β1 and β5 activities are significantly increased upon infection with pathogenic *Pseudomonas syringae* pv. *tomato* DC3000 lacking hopQ1-1 [PtoDC3000(ΔhQ)] whilst the activity profile of the β1 subunit changes. Infection with wild-type PtoDC3000 causes proteasome activities that range from strongly induced β1 and β5 activities to strongly suppressed β5 activities, revealing that β1 and β5 activities can be uncoupled during bacterial infection. These selective probes and inhibitors are now available to the plant science community, and can be widely and easily applied to study the activity and role of the different catalytic subunits of the proteasome in different plant species.

Keywords: catalytic subunit, core protease, *Arabidopsis thaliana*, *Nicotiana benthamiana*, activity-based protein profiling, proteasome manipulation, technical advance.

INTRODUCTION

The ubiquitin proteasome pathway is responsible for the selective degradation of proteins in the cell regulating numerous cellular and physiological functions. The proteasome is a multi-subunit, ATP-dependent proteolytic complex consisting of a 20S core particle (CP) and a 19S regulatory particle (RP; Groll *et al.*, 1997). The CP is ubiquitin and ATP independent, and consists of four stacked rings forming a barrel. The inner two rings of the barrel

consist of β subunits and these are flanked by two rings of α subunits (Kurepa and Smalle, 2008a). Each ring consists of seven subunits. The catalytic subunits responsible for peptide cleavage are located in the β rings and have an active site N-terminal threonine (Thr). The catalytic β subunits have different proteolytic activities: β1 has caspase-like activity; β2 trypsin-like activity; and β5 chymotrypsin-like activity (Dick *et al.*, 1998).

In addition to its crucial role in plant hormone signaling, the ubiquitin proteasome pathway has received attention in the plant pathogen field because several pathogens target this system. The proteasome acts as a hub in various immune signaling cascades, and is therefore an obvious target for pathogens (Üstün *et al.*, 2016). Pathogen-derived effectors were found to interact with components of the ubiquitin proteasome system, such as E3-ligases, F-box proteins and SUMO de-conjugation enzymes (Banfield, 2015). These effectors interfere in vesicle trafficking or promote transcription factor degradation. Some of these bacterial effectors act by inhibiting the proteasome. For instance, the XopJ effector produced by *Xanthomonas campestris* pv. *vesicatoria* and the HopZ4 effector from *Pseudomonas syringae* pv. *lachrymans* interact with the RPT6 subunit of the 19S RP, suppressing the activity of the proteasome and repressing salicylic acid (SA)-mediated responses (Üstün *et al.*, 2013, 2014). In addition, the non-ribosomal polypeptide syringolin A (SylA) secreted by *P. syringae* pv. *syringae* also targets the proteasome (Groll *et al.*, 2008), in this case by covalently inhibiting β2 and β5 subunits of the plant proteasome (Kolodziejek *et al.*, 2011). SylA facilitates opening of stomata and promotes bacterial colonization from wound sites (Schellenberg *et al.*, 2010; Misas-Villamil *et al.*, 2013).

So far, the plant proteasome could not be sufficiently investigated due to technical limitations and lack of suitable approaches. First, reverse genetic approaches are challenging as mutations in CP subunits usually cause severe pleiotropic defects or even lethality (Kurepa and Smalle, 2008a). Roles of the different CP subunits are also impossible to study using a knockout approach as the CP requires integrity for its function. Second, a number of proteasome subunits are modified post-translationally, for example, by proteolytic processing, acetylation and ubiquitylation (Book *et al.*, 2010). Third, the proteasome is a versatile complex in which substrate specificities can be changed, depending on the assembly of the different subunits. The most notable example is the immunoproteasome in mammals in which constitutive subunits of the CP are replaced by inducible subunits (Aki *et al.*, 1994). The recently discovered replacement of α3 by α4 in human proteasomes is another example of alternative proteasomes (Padmanabhan *et al.*, 2016). Although there is no evidence that plants have an alternative proteasome, plant genomes carry multiple genes for nearly each subunit (Yang *et al.*, 2004), and the proteasome in Arabidopsis is assembled with paralogous pairs for most subunits (Book *et al.*, 2010). Remarkably, tobacco genes encoding β1, α3 and α6 subunits are transcriptionally upregulated after treatment with the elicitor cryptogein (Suty *et al.*, 2003), indicating that plants might assemble inducible alternative proteasomes.

The activity of the proteasome subunits can be studied using fluorogenic substrates, which require the isolation and purification of the proteasome, a very tedious and laborious method only applicable on certain soft plant tissues (Yang *et al.*, 2004; Book *et al.*, 2010). We previously introduced activity-based protein profiling (ABPP) to monitor the activity of the plant proteasome (Gu *et al.*, 2010). ABPP relies on the use of small molecule chemical probes that are composed of a reactive group, a linker and a reporter tag that can be biotin or fluorescent to facilitate protein purification and detection, respectively (Cravatt *et al.*, 2008). These chemical probes react with the active site of enzymes, resulting in a covalent and often irreversible labeling, which facilitates the detection, purification and identification of those labeled proteins. Labeling reflects protein activity rather than abundance because the probes only react when the active site is available and reactive, and many enzymes are regulated by changes in the availability and reactivity of the active site. So far we have introduced over 40 activity-based probes into plant science to monitor, for example, Cys proteases, glycosidases, subtilases, acyltransferases and glutathione transfereases, and many of these probes are widely used in plant science (Morimoto and van der Hoorn, 2016). DCG-04, for instance, is a probe for papain-like Cys proteases (Greenbaum *et al.*, 2000; van der Hoorn *et al.*, 2004) that has been instrumental for the discovery of pathogen-derived inhibitors (Rooney *et al.*, 2005; Tian *et al.*, 2007; Shabab *et al.*, 2008; Van Esse *et al.*, 2008; Song *et al.*, 2009; Kaschani *et al.*, 2010; Lozano-Torres *et al.*, 2012; Mueller *et al.*, 2013), deciphering protease-inhibitor arms-races and effector adaptation upon a host jump (Hörger *et al.*, 2012; Dong *et al.*, 2014), and identifying senescence-associated proteases (Martínez *et al.*, 2007; Carrión *et al.*, 2013; Poret *et al.*, 2016;). Likewise, proteasome probes have been used to describe post-translational activation of the proteasome during SA signaling (Gu *et al.*, 2010); the selective suppression of the nuclear proteasome by bacterial phytotoxin SylA (Kolodziejek *et al.*, 2011; Misas-Villamil *et al.*, 2013); and the regulation of the proteasome by NAC transcription factor RPX (Nguyen *et al.*, 2013), the validation and availability of next-generation chemical probes will underpin exciting scientific discoveries.

The activity of the three catalytic subunits of the Arabidopsis proteasome can be easily distinguished using ABPP as these subunits have different molecular weight (MW; Gu *et al.*, 2010; Kolodziejek *et al.*, 2011). In other plants, however, the MW of these different subunits can

overlap, and multiple subunit genes can cause additional signals that are difficult to annotate (Gu, 2009). In the model plant *Nicotiana benthamiana*, for instance, all three different catalytic subunits were detected in a single band (Misas-Villamil *et al.*, 2013). Here, we describe subunit-specific labeling for two catalytic subunits. By using these next-generation probes we are able to display activities of β1 and β5 catalytic subunits in *N. benthamiana*, revealing that activity of these subunits independently changes upon bacterial infection.

RESULTS

LW124 and MVB127 are selective probes for the β1 and β5 catalytic subunits

We have previously used MVB072 (Figure 1a), a probe that labels all three catalytic subunits of the plant proteasome (Kolodziejek *et al.*, 2011). Labeling of Arabidopsis leaf extracts with MVB072 results in three signals representing β2 (top band 1), β5 (middle band 2) and β1 (bottom band 3; Figure 1b; Kolodziejek *et al.*, 2011). We also have previously introduced a rhodamine-tagged SylA (RhSylA; Figure 1a) that preferentially labels β2 (top band 6) and β5 (bottom band 7; Figure 1b; Kolodziejek *et al.*, 2011).

Here we introduce two next-generation probes for labeling of specific proteasome catalytic subunits. LW124 contains an epoxyketone reactive group, the tetrapeptide Ala-Pro-Nle-Leu and a bodipy Cy2 fluorescent group (Figure 1a; Li *et al.*, 2013). MVB127 has a vinyl sulfone (VS) reactive group, a MeTyr-Phe-Ile tripeptide and a bodipy Cy2 fluorescent group with an azide group that can be used for click chemistry reactions (Figure 1a; Li *et al.*, 2013). In contrast to MVB072 labeling, which in Arabidopsis results in three signals, we detect only one signal for LW124 at 26 kDa (Figure 1b; band 4), and one signal for MVB127 at about 27 kDa (Figure 1b; band 5). No strong signals appear in the remainder of the gels (Figure S1). All signals are caused by proteasome labeling as they are suppressed upon pre-incubation with the selective proteasome inhibitor epoxomicin (Figure S2).

Because LW124 carries a different fluorophore, we tested if these probes can be mixed and used in co-labeling experiments. Co-labeling by adding two probes at the same time and with the same concentration to Arabidopsis

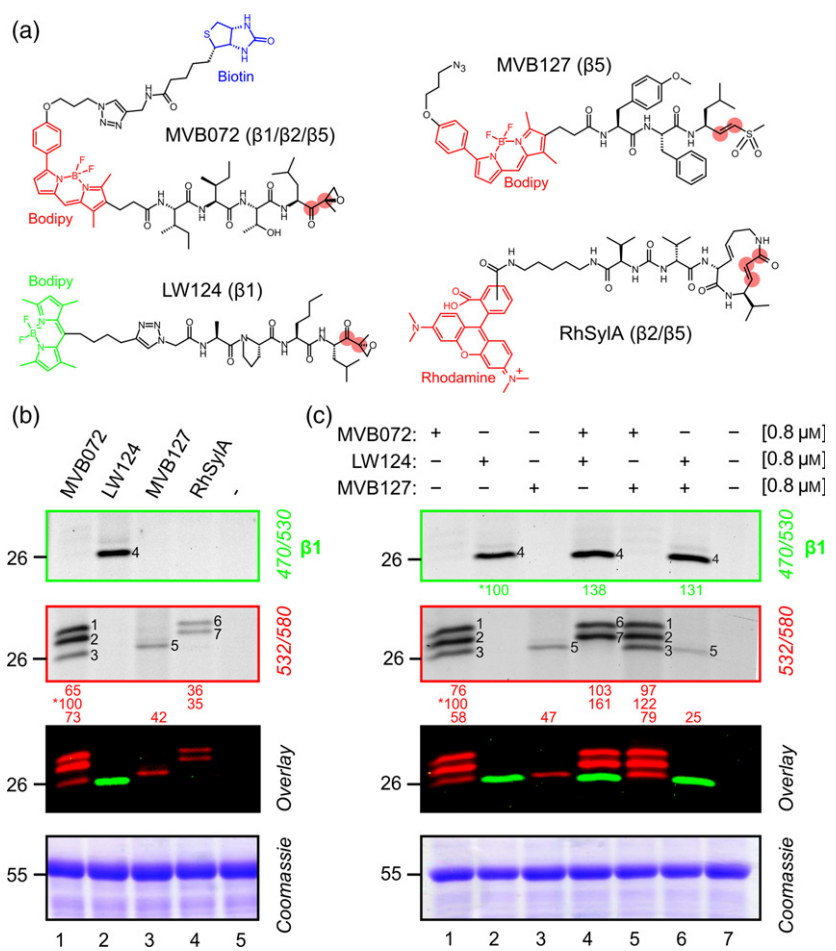

Figure 1. Subunit-specific labeling of Arabidopsis proteasome catalytic subunits.
(a) Structures of probes used in this study. MVB072 carries an epoxyketone reactive group, a Ile-Ile-Ser-Leu tetrapeptide mimic and both a Bodipy TAMRA fluorophore (ex532/em580, red) and a biotin affinity handle. LW124 contains an epoxyketone reactive group on a Ala-Pro-Nle-Leu tetrapeptide mimic and a Bodipy Cy2 fluorophore (ex470/em530). MVB127 carries a vinyl sulfone (VS) reactive group, a MeTyr-Phe-Ile tripeptide, and both an azide minitag and a Bodipy TAMRA fluorophore (ex532/em580). Rhodamine-tagged syringolin A (RhSylA) contains a Michael system reactive group embedded in a SylA structure and carries a rhodamine fluorophore (ex532/em580, red). Sites that are targeted by the catalytic Thr of the proteasome are highlighted with circles.
(b) Comparison of the different labeling profiles generated with the four different probes. Arabidopsis leaf extracts were labeled at pH 7.5 with 0.8 μM MVB072, LW124 and MVB127 for 2 h, and with 0.5 μM RhSylA for 30 min. Fluorescent proteins were detected by in-gel fluorescent scanning at two indicated settings. Numbers on the gel annotate signals caused by the labeled proteins. Numbers below the gels show the intensity of the fluorescent signals, as a percentage compared with the reference signal indicated by an asterisk. See Figure S1 for entire gels. This experiment was performed at least three independent times with similar results.
(c) (Co)labeling of proteasome subunits with the different probes. Arabidopsis leaf extracts were (co) labeled with MVB072, LW124, MVB127 for 2 h. Fluorescent proteins were detected as described in (b). This experiment has been reproduced at least three independent times with similar results.

leaf extracts indeed shows specific signals for both probes (Figure 1c). The bottom signal (band 3, β1) of MVB072 is suppressed upon co-labeling with LW124 (Figure 1c; lane 4), indicating that LW124 targets β1 of the Arabidopis proteasome. The overlay shows that the β1-LW124 conjugate (band 4) migrates slightly faster in the protein gel than the β1-MVB072 conjugate (band 3), consistent with the different MWs of the two probes (Figure 1b and c; lanes 1 and 2). A suppression of labeling cannot be observed upon co-labeling of MVB072 with MVB127 as they carry the same fluorophore (Figure 1c; lane 5). Co-labeling of LW124 with MVB127 results in two signals (Figure 1c; top two panels, lane 6), indicating that these probes label different subunits. However, the MVB127 signal (band 5) is suppressed upon co-labeling with LW124 (Figure 1c; lanes 3 and 6). By contrast, labeling by LW124 (band 4) seems unaffected upon co-labeling with MVB127 (Figure 1c; lanes 2 and 6).

To confirm that LW124 and MVB127 are specific probes for one proteasome catalytic subunit, we pre-incubated the samples with subunit-specific proteasome inhibitors that have been validated on mammalian proteasomes. N3β1 is an epoxyketone inhibitor that targets the β1 catalytic subunit, whereas N3β5 is a VS inhibitor of the β5 catalytic subunit (Figure 2a; Verdoes *et al.*, 2010). Notably, these are non-fluorescent versions of the probes as the peptide and reactive group (warhead) of N3β1 is identical to that of LW124, and the warhead of N3β5 is identical to that of MVB127 (Figures 1a and 2a). Pre-incubation with N3β1 suppresses labeling of only the bottom band 3 in the MVB072 labeling profile, confirming that this inhibitor is selective for the β1 subunit (Figure 2b; lane 2). By contrast, pre-incubation with N3β5 suppresses MVB072 labeling of the middle band 2, confirming selectivity for β5 (Figure 2b; lane 3).

Having verified the selectivity of N3β1 and N3β5, we tested if LW124 and MVB127 labeling can be supressed by the respective subunit-selective inhibitor. N3β1 suppresses labeling of LW124 (Figure 2b; lanes 5 and 8), confirming that LW124 targets β1, consistent with the structural similarity of LW124 with N3β1 (Figures 1a and 2a). Importantly, the suppression of MVB127 labeling by N3β5 (Figure 2b; lanes 6 and 12) shows that MVB127 targets β5, consistent with the structural similarity of MVB127 with N3β5 (Figures 1a and 2a). The β5-MVB127 conjugate (band 5) migrates slightly faster in the protein gel than the β5-MVB072 conjugate (band 2), consistent with the

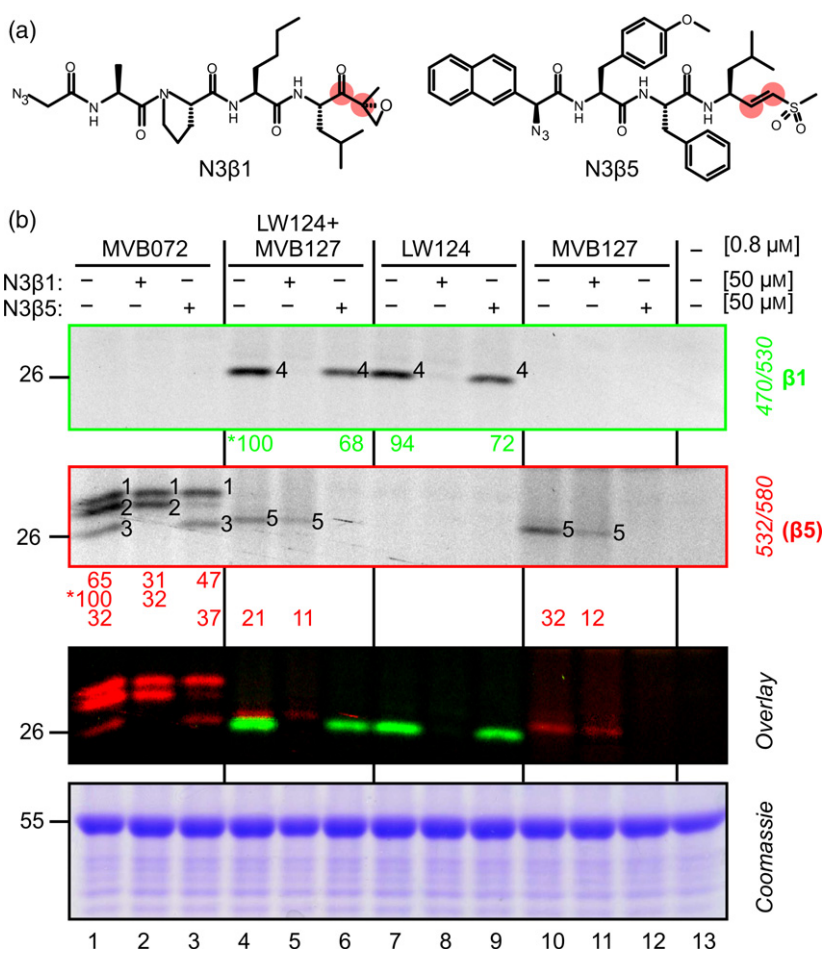

Figure 2. Subunit-selective inhibitors confirm selective subunit labeling.
(a) Structures of specific inhibitors for the β1 and β5 proteasome catalytic subunits. N3β1 is an epoxyketone specific inhibitor of the β1 catalytic subunit of the proteasome. N3β5 is a vinyl sulfone (VS)-based inhibitor that specifically targets the β5 catalytic subunit of the proteasome. Both inhibitors contain an azide group. Reactive groups are indicated with circles.
(b) Subunit-specific inhibitors confirm subunit-selective labeling by LW124 and MVB127. Arabidopsis leaf extracts were pre-incubated with 50 μM N3β1 or N3β5 for 30 min, followed by (co)labeling with MVB072, LW124 and MVB127 for 2 h. Fluorescent proteins were detected and annotated with numbers as described in Figure 1b. The experiment has been reproduced three independent times with similar results.

different MWs of the two probes (Figure 1b and c; lanes 1 and 3; Figure 2b; lanes 1 and 4). Importantly, pre-incubation of N3β1 or N3β5 in the reciprocal combinations with the probes did only slightly reduce MVB127 and LW124 labeling, respectively (Figure 2b; lanes 5, 6, 9 and 11), indicating that both inhibitors and probes are specific for their targets. Taken together these data show that LW124 and MVB127 are selective probes for β1 and β5 catalytic subunits, respectively.

Specific labeling of the β2 catalytic subunit

Having established selective labeling of the β1 and β5 catalytic subunits, we next developed a method to monitor β2. We previously found that RhSylA targets the proteasome subunits β2 and β5 at short labeling times (Kolodziejek *et al.*, 2011). Taking advantage of this feature we tested if inhibition of the β5 proteasome subunit using N3β5 together with short labeling by RhSylA will result in specific labeling of β2. We therefore pre-incubated Arabidopsis leaf extracts with various concentrations of N3β5 and labeled for 30 min with 0.5 μM RhSylA. Increasing N3β5 concentrations up to 5 μM N3β5 reduces β5 labeling (Figure 3a and b). β5 labeling remains unaltered at higher N3β5 concentrations (Figure 3a and b), indicating that β5 subunit is saturated by N3β5. Signal intensities derived from β1 and β5 at 5 μM N3β5 are very faint in comparison to the β2 signal, which remains unaffected (Figure 3b). These data, and its replicate (Figure S3), demonstrate that RhSylA labeling in the presence of 5 μM N3β5 is a suitable approach to monitor labeling of β2.

Subunit-specific probes display multiple β1 signals in *Nicotiana benthamiana*

Nicotiana benthamiana is increasingly used as a model plant to study protein regulation and localization upon transient expression. Additionally, *N. benthamiana* can be infected by a range of different pathogens, which makes this species ideal to unravel plant defense (Goodin *et al.*, 2008). Labeling of *N. benthamiana* leaf extracts with MVB072 results in two signals: one strong signal at 28 kDa; and one faint signal at about 27 kDa (Figure 4a; lane 1, bands 1 and 2; Misas-Villamil *et al.*, 2013). Mass spectrometry (MS) analysis of the MVB072-labeled proteins representing the major signal revealed that it contains β1, β2 and β5 subunits (Misas-Villamil *et al.*, 2013). Thus, in contrast to Arabidopsis where the three catalytic subunits cause three distinct signals, the *N. benthamiana* proteasome subunits cannot be distinguished by MVB072 labeling because the signals overlap.

To monitor the catalytic subunits of the *N. benthamiana* proteasome, we tested the subunit-selective probes. Surprisingly, LW124 labeling displays two 27 kDa signals, indicating that there might be two different subunits labeled by LW124 in *N. benthamiana* (Figure 4a; lane 2, bands 3 and 4). Co-labeling of MVB072 with LW124 shows two signals for LW124 and one signal for MVB072 (Figure 4a; lane 4 overlay). The weak bottom MVB072 signal (band 2) is absent upon co-labeling with LW124, indicating that this signal is caused by β1. Because the top MVB072 signal (band 1) also contains β1 (Misas-Villamil *et al.*, 2013), both MVB072 signals contain β1, consistent with the two signals displayed by LW124. The overlay, however, shows that the two MVB072 signals migrate slower in the gel than the two LW124 conjugates (Figure 4a; lanes 1 and 2), which is consistent with the MW shift seen for Arabidopsis, and is explained from the fact that MVB072 is larger and more bulkier when compared with LW124 (Figures 1a and 2a).

MVB127 labeling shows one specific signal at 28 kDa (Figure 4a; lane 3, band 5). Co-labeling of MVB072 with MVB127 causes a more intense bottom signal, caused by an overlap of the β1-MVB072 and β5-MVB127 conjugates. The observation that the β5-MVB127 conjugate migrates

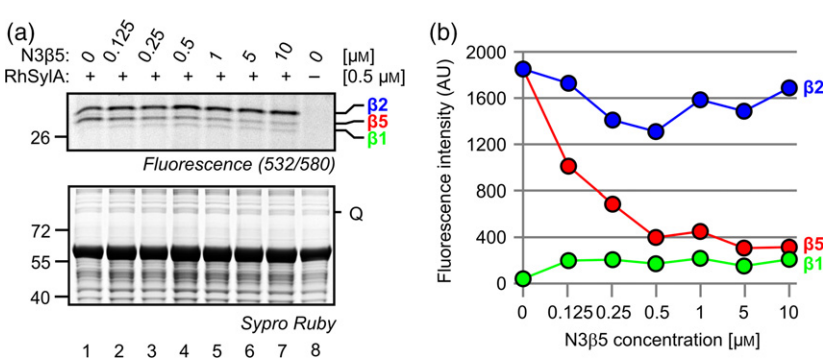

Figure 3. Selective β2 labeling using [RhSylA + N3β5].
(a) In the presence of N3β5, rhodamine-tagged syringolin A (RhSylA) labels β2 selectively. Arabidopsis leaf extracts were pre-incubated with increasing concentrations of the β5 selective inhibitor N3β5 for 15 min followed by labeling with 0.5 μM RhSylA for 30 min. Proteins were detected by in-gel fluorescent scanning and Sypro Ruby staining. This experiment has been repeated four independent times with similar results.
(b) Quantification of fluorescence labeling. Fluorescent signals corresponding to the catalytic subunits β1, β2 and β5 were quantified from fluorescent gels. Fluorescence intensity values were normalized for loading using the Sypro Ruby signal Q, indicated in (a). Values for the catalytic subunits were plotted against different N3β5 concentrations. A reproduction of this experiment is shown as Figure S3.

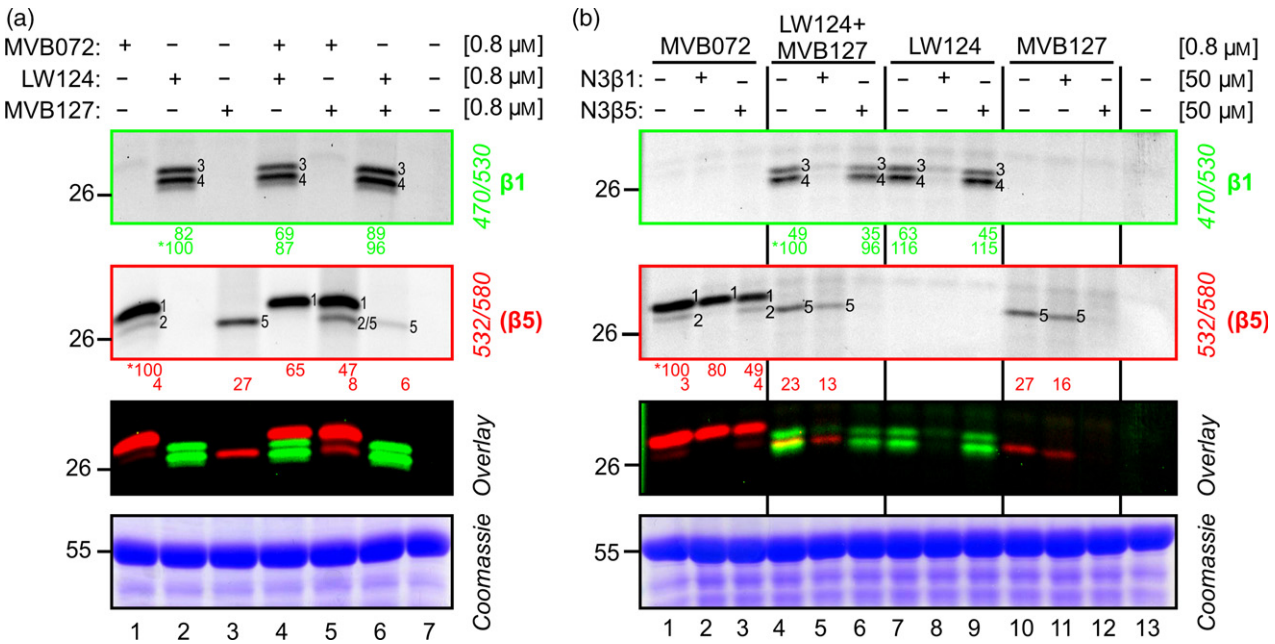

Figure 4. Labeling of *Nicotiana benthamiana* proteasome with subunit-specific probes.
(a) Labeling profiling of proteasome specific probes. *Nicotiana benthamiana* leaves extracts were (co)labeled at pH 7.5 with 0.8 μM MVB072, LW124 and MVB127 for 2 h. Fluorescent proteins were detected as described in Figure 1b. Numbers on gels annotate the different signals caused by labeled proteasome subunits. This experiment has been reproduced at least three independent times with similar results.
(b) Selective (co)labeling of β1 and β5 of *N. benthamiana*. *Nicotiana benthamiana* extracts were pre-incubated with 50 μM of the selective proteasome inhibitors N3β1 and N3β5 for 30 min followed by 2 h (co)labeling with 0.8 μM MVB072, LW124 and MVB127. Fluorescent proteins were detected as described in Figure 1b. Shown is a representative gel of three independent biological replicates.

faster through the protein gel than the β5-MVB127 conjugate is consistent with the MW shift seen for Arabidopsis, and is explained from the fact that MVB072 is larger and more bulkier when compared with MVB127 (Figures 1a and 2a). LW124 and MVB127 co-labeling results in two signals for LW124 and one signal for MVB127 (Figure 4a; lane 6).

Pre-incubation with N3β1 and N3β5 confirms that the lowest MVB072 signal (Figure 4b; band 2) and the two LW124 correspond to β1 (Figure 4b; bands 3 and 4), whereas the MVB127 signal corresponds to β5 (Figure 4b; band 5), supporting the specificity of β1 and β5 labeling by LW124 and MVB127, respectively (Figure 4b; lanes 5–12). There is, however, some reciprocal suppresion of N3β1 on MVB127(β5) and N3β5 on LW124(β5) (Figure 4b; lanes 5, 6, 9 and 11).

Phylogenetic and proteomic analysis reveals multiple incorporated proteasome subunits in *Nicotiana benthamiana*

The detection of two β1 signals in *N. benthamiana* using LW124 is remarkable, as the Arabidopsis genome has only one gene encoding β1, and *β1din* in tobacco is defence induced (Suty *et al.*, 2003). We therefore searched the *N. benthamiana* genome (https://solgenomics.net/) for genes encoding catalytic subunits of the proteasome. Blast searches for catalytic subunits resulted in six predicted β1 proteins, three β2 proteins and three β5 proteins. Phylogenetic analysis revealed that the paralogous subunits are more related to each other than to the subunits of Arabidopsis, except for β1, where two groups seem to exist in *N. benthamiana* (Figure 5). One β1 and one β2 subunit are shorter than their respective paralogs. We consider these pseudogenes as their predicted MW is too low to explain the signals we detect upon labeling.

To determine if these genes also encode for proteins that are part of the active proteasome in leaves, we performed MS analysis of two different pull-down experiments of *N. benthamiana* leaf extracts labeled with MVB072. To also detect an altered subunit assembly during defence, the pull-down was performed on plants treated with the SA analog benzothiadiazole (BTH), whereas the other pull-down was performed on the mock control. Each pull-down assay was analyzed twice by MS and 45 peptides were detected of the catalytic subunits, of which 11 were unique (Figure S4; Table S1).

In these experiments we identified unique peptides of two different β1 subunits: β1a and β1b (Figure 5b and c, and S2). Several peptides that are shared with one other protein (dark gray) map to the truncated β1 subunit (NbS00011733g0005.1; dark gray in Figure 5c). The

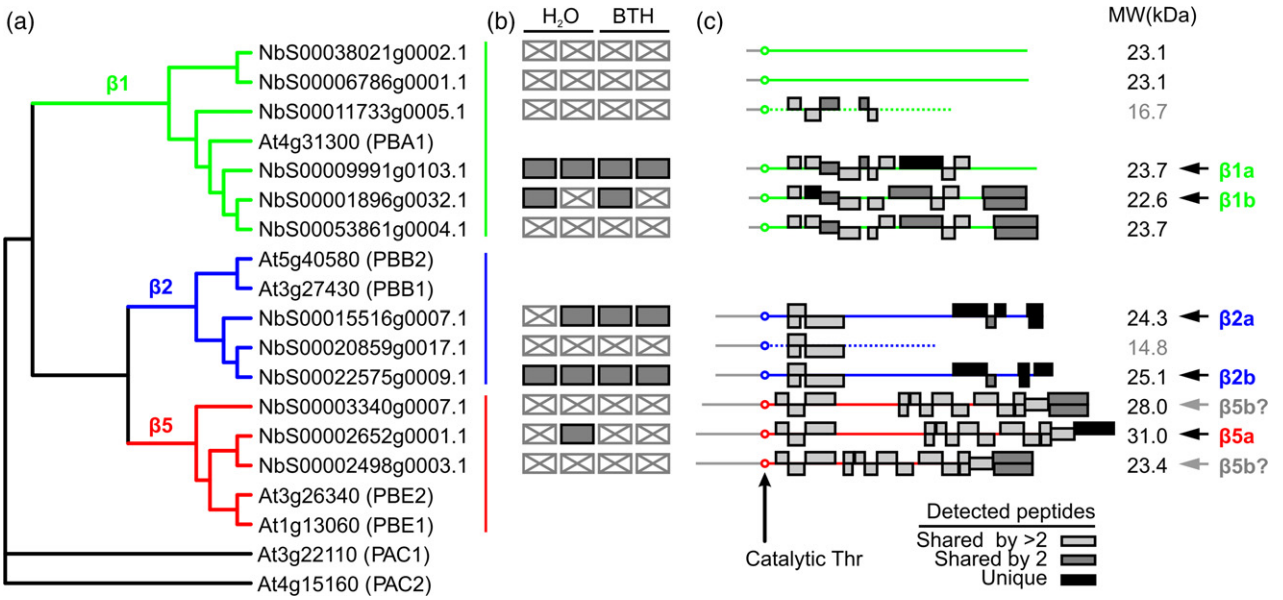

Figure 5. Detection of the expanded proteasome subunit repertoire of *Nicotiana benthamiana*.
(a) Neighbor-joining phylogenetic tree of β1, β2 and β5 catalytic subunits of the proteasome of Arabidopsis and *N. benthamiana*, rooted with the α3 subunit (PAC1 and PAC2).
(b) Identification of unique peptides upon MVB072 pull-down from *N. benthamiana* leaf extracts. Leaf extracts from plants treated with water or benzothiadiazole (BTH) were labeled with MVB072, and the labeled proteins purified on avidin beads, eluted and separated on protein gels. Proteins were digested in-gel with trypsin and the eluted peptides were analyzed twice by mass spectrometry (MS). Filled gray boxes indicate the detection of unique peptides of the respective proteasome subunit, whereas crossed boxes indicate no unique peptides detected.
(c) Position of detected peptides of the catalytic subunits. Shown are the peptides that are unique (black); shared with one other subunit (dark gray); or shared with more than one subunit (light gray). Gray lines indicate the propeptide that is removed upon proteasome assembly. The mature protein starts with a catalytic Thr residue. Truncated β1 and β2 proteasome subunits that may not be functional are shown as dashed lines. The molecular weight (MW) indicates the calculated MW of the mature subunit (without propeptide) in kDa. Black arrows indicate subunits that were identified with unique peptide(s), and the gray arrow indicates the identified β5 subunit, in case the truncated β5 subunit is considered non-functional.

truncated subunit would migrate at a predicted 16.7 kDa, but we do not detect fluorescent signals in this region. Removal of this subunit from the analysis would add two additional unique peptides to one of the already identified β1a subunits (NbS0009991g0103.1). The presence of two β1 subunits having a different predicted MW of 23.7 (β1a) and 22.6 (β1b) kDa is consistent with the two LW124 signals detected upon labeling.

We also detected unique peptides for two β2 subunits (β2a and β2b) and one β5 subunit (β5a) (Figure 5b). Two other β5 subunit peptides do not match to this identified β5a protein, indicating that there must be a second β5 subunit (β5b), which is either Nb00003340g0007.1 or the shorter NbS00002498g0003.1 (Figure 5b and c). These findings confirm an expanded repertoire of catalytic proteasome subunits in active proteasomes of *N. benthamiana*.

Comparison of the identified proteasome subunits from water- and BTH-treated plants did not reveal significant differences (Figure 5b). These data suggest that the active catalytic proteasome subunit incorporation is not different during SA-induced defence. However, more quantitative proteomic analysis with more samples may be required to rule out any changes upon BTH treatment.

Bacterial infections affect active subunit compositon in *Nicotiana benthamiana*

We next used the subunit-selective probes to investigate changes in the proteasome subunit composition during biotic stress. We therefore infected *N. benthamiana* leaves with *P. syringae* pv. *tomato* DC3000 (PtoDC3000), which triggeres a non-host response [NHR; or effector-triggered immunity (ETI)] because it produces type-III effector hopQ1-1, which is recognized in *N. benthamiana*. We also included the ΔhopQ1-1 mutant of PtoDC3000 [PtoDC3000 (ΔhQ)], which causes disease on *N. benthamiana* (Wei *et al.*, 2007).

Unexpectedly, whilst the proteasome labeling upon infection with PtoDC3000(ΔhQ) is highly reproducible, we noticed that proteasome labeling upon infection with PtoDC3000(WT) differs significantly between eight independent infection assays. MVB072 labeling of extracts of PtoDC3000(WT)-infected leaves indicates that the activity of the proteasome is either upregulated (Figure 6a) or downregulated (Figure 6b). Importantly, labeling the same extracts with LW124 + MVB127 provides more information. The lower β1 signal either intensifies strongly upon PtoDC3000(WT) infection (Figures 6c, and S5 and S6), or

only slightly (Figures 6d, and S7–S9). Remarkably, however, the β5 signal is either induced (Figures 6c, and S5 and S6) or strongly suppressed (Figures 6d, and S7–S9). The fact that the ratio between β1 and β5 can differ between infection experiments demonstrates that the activitites of these two subunits can be uncoupled during bacterial infection. The cause of this phenotypic variation upon PtoDC3000(WT) infection is beyond the focus of the current manuscript, and is subject to further studies.

Proteasome activities upon infection by PtoDC3000(ΔhQ) show a robust threefold upregulation in the intensity of the β1 and β5 signals (Figures 6e and S10). Quantitative reverse transcriptase-polymerase chain reaction (PCR) with gene-specific primers showed that also transcript levels of β1a, β1b and β5 are significantly upregulated (Figure 6f), indicating that the differential proteasome activitiy upon PtoDC3000 (ΔhQ) is mostly transcriptional. Notably, we detect a highly reproducible shift in the ratio between the two β1 signals upon infection with PtoDC3000(ΔhQ) (Figure 6g).

DISCUSSION

We have introduced next-generation subunit-specific probes for labeling the β1 and β5 proteasome catalytic subunits, and validated labeling in both *Arabidopsis thaliana* and *N. benthamiana*. We also introduced and validated subunit-selective inhibitors for the β1 and β5 subunits, which may be useful for chemical knockout assays. We discovered that the active *N. benthamiana* proteasome contains different paralogous catalytic subunits: two for β1, two for β2 and two for β5. Application of selective subunit labeling revealed and uncoupled induction in β1 and β5 subunits upon infection with virulent and avirulent *P. syringae*.

Our data demonstrate that LW124 targets β1 and MVB127 targets β5. Because the proteasome subunits of Arabidopsis have a distinct MW, we would have detected additional signals if LW124 and MVB127 would label additional catalytic subunits. Likewise, MVB127 should have caused an additional signal if it could label β1 of *N.*

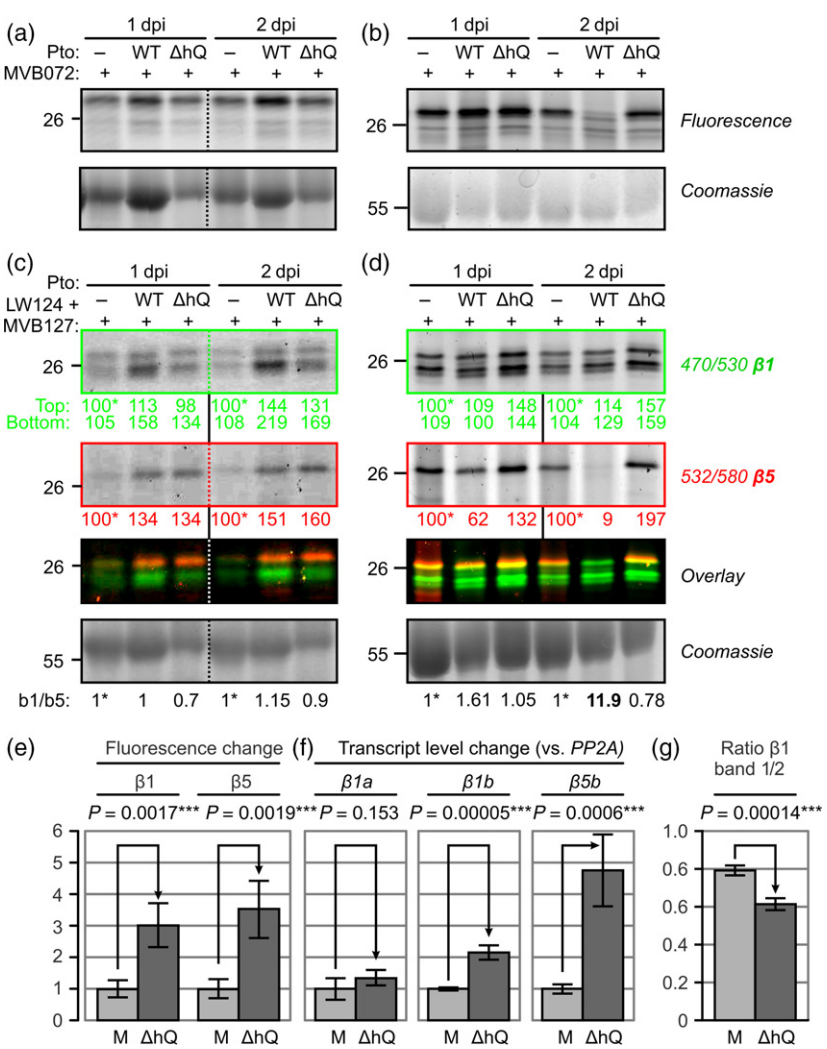

Figure 6. Uncoupled differential β1 and β5 activities upon bacterial infections.
(a–g) *Nicotiana benthamiana* leaves were infiltrated with buffer or 10^6 CFU ml^{-1} PtoDC3000(WT) or its derived *ΔhopQ1-1* mutant PtoDC3000(ΔhQ), and leaf disks were harvested at 1 and 2 dpi. Leaf extracts were labeled with MVB072 (a,b) or LW124 + MVB127 (c,d), and proteins were analyzed as described in Figure 1b. Shown are representatives of independent experiments showing the two different phenotypes, ranging from induced β1/β5 activities (a,c; Figures S5 and S6) to suppressed β5 activities (b,d; Figures S7–S9). (e) Quantified fluorescence for β1 (LW124) and β5 (MVB127) in one experiment with four individuals ($n = 4$ replicates). This experiment was reproduced twice with similar results (Figure S10). (f) Relative transcript levels of β1a, β1b and β5b relative to *PP2A* for the same experiment ($n = 4$ individual plants) as shown in (e). (g) Relative ratio of the two LW124 signals in the same experiment ($n = 4$ replicates) as shown in (e). This experiment was reproduced twice with similar results (Figure S10).

benthamiana. The absence of additional signals in Arabidopsis testifies the high selectivity of the subunit-selective probes.

By contrast, however, despite their structural similarity with the probes, the subunit-selective inhibitors partially suppress reciprocal labeling: N3β1 suppresses labeling of β5 by MVB127 and N3β5 suppresses labeling by LW124, in both Arabidopsis (Figure 2b) and *N. benthamiana* (Figure 4b). Likewise, we detect a consistent suppression of β5 labeling by MVB127 upon co-labeling with LW124 (Figures 1c, 2b, 4a and b). Although we can not exclude at this stage that N3β1 and N3β5 are weak inhibitors of β5 and β1, respectively, the fact that the coresponding probes are subunit-selective suggests an alternative explanation. The suppression of labeling by inhibitors and probes that target other subunits may also be caused by crowding of the proteolytic chamber (inhibitor bound to one subunit hinders access of probes to another subunit) or allosteric regulation (inhibition of one subunits affects labeling efficiency of another subunit). Although the proteolytic chamber is probably too large to support the crowded chamber hypothesis, the catalytic subunits of the proteasome are known to allosterically regulate each other, for example, to facilitate the cyclical bite-chew mechanism (Kisselev *et al.*, 1999).

Nicotiana benthamiana assembles different proteasomes

LW124 labeling of *N. benthamiana* displays two different β1 signals. MS analysis of MVB072-labeled proteins confirmed that at least two different β1 proteins are incorporated in proteasomes as active catalytic subunits. Subunits that are not incorporated into the proteasome remain in the inactive precursor state and are probably degraded (Chen and Hochstrasser, 1996). MS analysis of MVB072-labeled proteins also revealed at least two different β2 proteins and two different β5 subunits that must have been part of an active proteasome. However, MVB127 labeling only diplays one β5 signal, indicating that the labeled proteins run at the same height. The fact that multiple paralogs were identified demonstrates that *N. benthamiana* produces diverse catalytic subunits and might assemble different proteasomes.

The concept that plants can assemble multiple proteasomes is supported by the finding that Arabidopsis also incorporates paralogous subunits into the 26S proteasome (Yang *et al.*, 2004; Book *et al.*, 2010). Remarkably, little is known about the role of paralogous CP subunits but more about paralogous RP subunits. Different paralogs of a subunit may act redundantly. For example, the RPN1 subunit in Arabidopsis is encoded by two genes, *RPN1a* and *RPN1b,* which differ in their expression pattern (Yang *et al.*, 2004). Nevertheless, *rpn1a* mutant lines maintain a functional proteasome indicating a redundant function (Wang *et al.*, 2009). RPT2 and RPT5 isoforms also share redundant functions (Lee *et al.*, 2011). In both Arabidopsis and maize, RPT2 and RPT5 are encoded by the paralogous genes *RPT2a-RPT2b* and *RPT5a-RPT5b*, respectively (Book *et al.*, 2010). However, there are cases where paralogous subunits seem to have different functions. For example, *RPT5b* complements *RPT5a* in the *Col* ecotype, but not in *Ws* ecotype (Gallois *et al.*, 2009), demonstrating an ecotype-dependent redundancy but also indicating alternative functions for the different isoforms. *Nicotiana benthamiana* is an allotetraploid, and the ancient genome duplication may explain a duplication of the proteasome subunits genes. At this stage, it is unclear if the different paralogous proteins have different functions.

Modification of the proteasome upon bacterial infection

Interestingly, subunit-selective proteasome activity profiling revealed that the activity of the catalytic β5 subunit can be strongly induced or suppressed upon infection with *P. syringae* and show that the activities of β1 and β5 can be uncoupled during infection. Uncoupling is not expected for proteasome complexes that incorporate equal numbers of catalytic subunits, but may have been caused by selective subunit inhibition during infection with *P. syringae*, or the specific activation of the β1 subunit during NHR/ETI responses.

Mammals have inducible subunits that can replace other β subunits, for example, to create the immunoproteasome (Aki *et al.*, 1994). Immunoproteasomes exhibit modified peptidase activities and variable cleavage site preferences. Their main function is the maintenance of cell homeostasis and cell viability under oxidative conditions (Seifert *et al.*, 2010). It is likely that plants also possess a type of inducible proteasome where some catalytic subunits are replaced under biotic or abiotic stresses. We have identified six genes encoding β1 catalytic subunits from the *N. benthamiana* genome, suggesting that the other isoforms that we did not detect by MS analysis are either expressed under different conditions, are tissue specific or are pseudogenes. This can also be the case for non-identified β2 and β5 proteins. Induction of genes encoding α and β proteasome subunits has been described for tobacco cells treated with cryptogein (Dahan *et al.*, 2001), whereas our earlier study revealed a post-translational upregulation of proteasome labeling upon treatment of Arabidipsis with benzodiadiazole (Gu *et al.*, 2010). Transcript activation of proteasome genes after cryptogein treatment could be associated with oxidative stress, as attenuation of the oxidative burst blocks the expression of *β1din*, *α3din* and *α6din* genes (Suty *et al.*, 2003).

Thus, different paralogous proteasome subunits might be assembled in active proteasomes under different conditions, for instance responding to oxidative stress. The encoded catalytic subunits in *N. benthamiana* carry only few polymorphic amino acid residues, and it is unknown at

this stage to what extend they affect proteasome function, for example, with respect to substrate selection and conversion. This study uncovers that more research is needed to investigate the occurrence and function of alternative proteasomes in plants.

Taken together, we have introduced subunit-specific probes to monitor the β1 and β5 subunits of the plant proteasome. The use of site-specific probes combined with phylogenetic and proteomic analysis revealed multiple isoforms for the β subunits, indicating that different proteasomes co-exist in leaves. The subunit-selective probes revealed unexpected, uncoupled differential activities of β1 and β5 upon bacterial infection that raise exciting questions on the underlying mechanism and biological role in immunity.

EXPERIMENTAL PROCEDURES

Probes and inhibitors

The synthesis of LW124, MVB127, N3β1 and N3β5 has been described previously (Verdoes *et al.*, 2010; Li *et al.*, 2013). As with our previously introduced probes, aliquots of these chemicals are available upon request and frequent use may accelerate their commercial availability.

Plant material and labeling conditions

Arabidopsis thaliana ecotype Col-0 and *N. benthamiana* plants were grown in the greenhouse under a regime of 14 h light at 20°C. Three–five-week-old plants were used for labeling experiments. For *in vitro* labeling, leaves were ground in water containing 10 mM dithiothreitol (DTT) and extracts were cleared by centrifugation. Labeling was performed by incubating the protein extract in 60 μl buffer containing 66.7 mM Tris pH 7.5 and 0.5–0.8 μM probe for 2 h at room temperature (22–25°C) in the dark. After acetone precipitation, pellets were re-suspended in 40 μl 1× loading buffer and samples were separated on 12% sodium dodecyl sulfate gel. Inhibitory assays were performed by 30 min pre-incubation of protein extracts with 50 μM of the inhibitor of interest, followed by 2 h labeling. For *in vivo* inhibition of the proteasome, 50 μM of the inhibitor was infiltrated in *N. benthamiana* leaves using a syringe without a needle. After 6 h incubation at room temperature, a leaf disc (1.6 cm diameter) of the infiltrated area was collected and labeled with the probe of interest as described above. Labeled proteins were visualized by in-gel fluorescence scanning using a Typhoon FLA 9000 scanner (GE Healthcare, http://www.gelifesciences.com) with Ex473/Em530 nm for LW124 and Ex532/Em580 nm for MVB127, MVB072 and RhSylA. Fluorescent signals were quantified using ImageQuant 5.2 (GE Healthcare) with the rolling ball method for background correction. To confirm equal loading, Coomassie brilliant blue or SyproRuby (Invitrogen) staining was performed according to the instructions of the manufacturer. SyproRuby gels were fluorescent scanned (Ex472/Em580 nm) and used for loading correction in the quantification of fluorescent signals. Statistical significance was calculated with a Student's *t*-test of at least three replicates.

Large-scale pull-down assay

Large-scale pull-down experiments were performed once on plants treated with BTH and once on the water control. This material was generated by spraying 3–4-week old *N. benthamiana* plants with 0.13 mg ml^{-1} BTH (BION, Syngenta) containing 0.01% Silwet L-77 (Lehle Seeds) or sprayed with water containing the same concentration of Silwet L-77. Leaves were harvested 2 days after treatment. Forty-four leaf discs of 2.3 cm diameter were collected per sample and ground in a buffer containing 1 mM DTT and 67 mM Tris pH 7.5. After centrifugation, 10 ml of protein extract was used for labeling with 20 μM MVB072 or 2.5 μl dimethylsulfoxide. Samples were incubated at room temperature and in the dark with gentle shaking for 2 h. Labeling was stopped by precipitating total proteins via the chloroform/methanol precipitation method (Wessel and Flügge, 1984). Affinity purification and in-gel digestion was performed as described elsewhere (Chandrasekar *et al.*, 2014).

MS

Liquid chromatography (LC)-MS/MS experiments were performed on an Orbitrap Elite instrument (Thermo; Michalski *et al.*, 2012) that was coupled to an EASY-nLC 1000 LC system (Thermo). The LC was operated in the one-column mode. The analytical column was a fused silica capillary (75 μm × 15 cm) with an integrated PicoFrit emitter (New Objective) packed in-house with Reprosil-Pur 120 C18-AQ 1.9 μm resin (Dr. Maisch). The LC was equipped with two mobile phases: solvent A [0.1% formic acid (FA) in water] and solvent B (0.1% FA in acetonitrile). All solvents were of UPLC grade (Sigma). Peptides were directly loaded onto the analytical column with a maximum flow rate that would not exceed the set pressure limit of 800 bar (usually about 0.7–0.8 μl min^{-1}). Peptides were subsequently separated on the analytical column by running a 60 min or 120 min gradient of solvent A and solvent B (60 min runs: start with 2% B; gradient 2–10% B for 2.5 min; gradient 10–35% B for 45 min; gradient 35–45% B for 7.5 min; gradient 45–100% B for 2 min; and gradient 100% B for 3 min; 120 min runs: start with 2% B; gradient 2–10% B for 5 min; gradient 10–35% B for 90 min; gradient 35–45% B for 15 min; gradient 45–100% B for 4 min; and gradient 100% B for 6 min) at a flow rate of 300 nl min^{-1}. The MS was operated using Xcalibur software (version 2.2 SP1.48). The MS was set in the positive ion mode. Precursor ion scanning was performed in the Orbitrap analyzer (FTMS) in the scan range of *m/z* 300–1800 and at a resolution of 60 000 with the internal lock mass option turned on (lock mass was 445.120025 *m/z*, polysiloxane; Olsen *et al.*, 2005). Product ion spectra were recorded in a data-dependent fashion in the ion trap (ITMS) in a variable scan range and at a rapid scan rate. The ionization potential (spray voltage) was set to 1.8 kV. Peptides were analyzed using a repeating cycle consisting of a full precursor ion scan (1.0×10^6 ions or 200 ms) followed by 15 product ion scans (1.0×10^4 ions or 50 ms) where peptides are isolated based on their intensity in the full survey scan (threshold of 500 counts) for tandem mass spectrum (MS2) generation that permits peptide sequencing and identification. CID collision energy was set to 35% for the generation of MS2 spectra. For the 2 h gradient length the data-dependent decision tree option and supplemental activation was switched on. The electron-transfer dissociation reaction time was 100 ms. During MS2 data acquisition dynamic ion exclusion was set to 30 sec with a maximum list of excluded ions consisting of 500 members and a repeat count of one. Ion injection, time prediction, preview mode for the FTMS, monoisotopic precursor selection and charge state screening were enabled. Only charge states higher than 1 were considered for fragmentation.

Peptide and protein identification using MaxQuant

RAW spectra were submitted to an Andromeda (Cox *et al.*, 2011) search in MaxQuant (version 1.5.3.30) using the default settings

(Cox and Mann, 2008), match-between-runs was activated (Cox *et al.*, 2014), and MS/MS spectra data were searched against the in-house generated *N. benthamiana* database (78 729 entries). All searches included a contaminants database (as implemented in MaxQuant, 267 sequences). The contaminants database contains known MS contaminants and was included to estimate the level of contamination. Andromeda searches allowed oxidation of methionine residues (16 Da) and acetylation of protein N-terminus (42 Da) as dynamic modification and the static modification of cysteine (57 Da, alkylation with iodoacetamide). Enzyme specificity was set to 'Trypsin/P'. The instrument type in Andromeda searches was set to Orbitrap and the precursor mass tolerance was set to ±20 ppm (first search) and ±4.5 ppm (main search). The MS/MS match tolerance was set to ±0.5 Da. The peptide spectrum match FDR and the protein FDR were set to 0.01 (based on target-decoy approach). Minimum peptide length was seven amino acids. The minimum score for modified peptides was 40.

Extraction of proteasome-specific peptides

The peptide.txt output files from MaxQuant were loaded into Perseus v1.5.3.0. After removal of peptides matching to the reversed database and peptides matching to the contaminant database, the remaining peptides were annotated using an in-house annotation file (annotation.wOG.txt). Peptides annotated to be derived from the proteasome or a proteasome subunit were extracted (Table S1) and manually mapped to the individual proteasome sequences (Figure S2).

Database search and phylogenetic analysis

The *N. benthamiana* database (v. 0.4.4, 76 379 sequences) was downloaded from the SOL genomics network (https://solgenomics.net) and a blast search using Arabidopsis catalytic subunits as a template was performed. Additionally, *N. benthamiana* annotated T1 proteins found in the MEROPS database (https://merops.sanger.ac.uk) were compared with the hits obtained by the search with Arabidopsis orthologs. The sequences were aligned with ClustalX2 (Larkin *et al.*, 2007) standalone program. The alignment parameters were used as follows: the pair-wise alignment gap opening penalty 30 and gap extension penalty 0.75, whereas for multiple alignment gap opening penalty were set to 15 and gap extension penalty to 0.3. Finally, the output alignment file from the ClustalX2 was used to generate the tree in R (Paradis *et al.*, 2004; Charif and Lobry, 2007). The neighbor-joining algorithm was implemented in the script for the construction of the phylogenetic tree from the calculated distance matrix.

Bacterial infections

For *P. syringae* infection, leaves of 5-week-old *N. benthamiana* plants were infiltrated using a needle-less syringe with 10^6 CFU ml^{-1} *P. syringae* pv. *tomato* DC3000 and its *ΔhopQ1-1* mutant derivative (Wei *et al.*, 2007). Three leaf discs (d = 1 cm) were harvested at days 1 and 2. Leaf extracts were generated in 200 μl of 50 mM Tris buffer at pH 7.5 containing 5 mM DTT, cleared by centrifugation and labeled for 2 h with 0.2 μM MVB072 or 0.8 μM LW124 + 0.8 μM MVB127 at room temperature in the dark in 50 μl total volume.

Nucleic acid preparation, cDNA synthesis and qRT-PCR

For RNA extraction, leaf material of *N. benthamiana*-infected leaves was frozen in liquid nitrogen, ground to powder. The RNA was extracted using Trizol (Ambion), treated with DNase (QIAGEN), purified using the RNeasy Plant Mini Kit (QIAGEN) and used the SuperScriptTM III Reverse Transcriptase (Invitrogen) for cDNA synthesis. The first-strand cDNA synthesis kit was used to reverse transcribe 1 μg of total RNA with oligo(dT) primers. The quantitative reverse transcriptase (qRT-PCR) analysis was performed using the iQ SYBR Green Supermix (Bio-Rad) with an iCycler (Bio-Rad). Specific primers were used to amplify β1a (forward: 5′-ctgctggatattgtgcctgc-3′; reverse: 5′-ggctcaaacatgtcgacagt-3′), β1b (forward: 5′-tgcccctattcacgtgtttg-3′; reverse: 5′-gttgcagcaggacaaaagga-3′), β5b (forward: 5′-ctcccattctacgtgcgtca-3′; reverse: 5′-ggattgacttgcctagctcac-3′) and *PP2A* (forward: 5′-gaccctgatgttgatgttcgct-3′; reverse: 5′-gagggatttgaagagagatttc-3′) was used as reference gene for normalization. Cycling conditions were as follows: 3 min at 95°C, followed by 45 cycles of 15 sec at 95°C, 15 sec at 60°C and 30 sec at 72°C. After each PCR, the specificity of the amplified product was verified with the melting curves. Gene expression levels for β1a, β1b and β5a were then calculated relative to *PP2A* using the $2-\Delta Ct$ (cycle threshold) method (Livak and Schmittgen, 2001). The average expression and the standard deviation of one experiment with four individuals were calculated, and expression of the mock control was set to 1. *P*-values were calculated using a two-tails *t*-test with unequal variance. *P*-values <0.0005 were marked with three asterisks.

ACKNOWLEDGEMENTS

The authors would like to thank Prof. Gunther Doehleman and Prof. George Coupland for their support. The authors are grateful to Prof. Collmer for providing the ΔhopQ1-1 mutant of PtoDC3000. This work was financially supported by the Max Planck Society, ERC Consolidator grant (R.H., grant No. 616449 'GreenProteases'), an ERC starting grant (M.K., grant No. 258413), the Deutsche Forschungsgemeinschaft (M.K., grant no. INST 20876/127-1 FUGG) and the University of Oxford.

CONFLICT OF INTEREST

The authors declare no conflict of interest.

SUPPORTING INFORMATION

Additional Supporting Information may be found in the online version of this article.

Figure S1. Entire gel showing selective labeling by different proteasome probes.

Figure S2. Labeling is blocked by pre-incubation with epoxomicin.

Figure S3. Selective β2 labeling using [RhSylA + N3β5].

Figure S4. Identified peptides mapped on the protein sequences of the catalytic subunits of the *Nicotiana benthamiana* proteasome.

Figure S5. Increased proteasome activity upon WT infection.

Figure S6. Increased proteasome activity upon WT infection.

Figure S7. Suppressed β5 labeling upon WT infection.

Figure S8. Suppressed β5 labeling upon WT infection.

Figure S9. Suppressed β5 labeling upon WT infection.

Figure S10. Altered proteasome activity upon infection with PtoDC3000(ΔhQ).

Table S1. Identified peptides of catalytic subunits.

REFERENCES

Aki, M., Shimbara, N., Takashina, M., Akiyama, K., Kagawa, S., Tamura, T., Tanahashi, N., Yoshimura, T., Tanaka, K. and Ichihara, A. (1994) Interferon-gamma induces different subunit organizations and functional diversity of proteasomes. *J. Biochem.* **115**, 257–269.

Banfield, M.J. (2015) Perturbation of host ubiquitin systems by plant pathogen/pest effector proteins. *Cell. Microbiol.* **17**, 18–25.

Book, A.J., Gladman, N.P., Lee, S.S., Scalf, M., Smith, L.M. and Vierstra, R.D. (2010) Affinity purification of the Arabidopsis 26S proteasome reveals a diverse array of plant proteolytic complexes. *J. Biol. Chem.* **285**, 25554–25569.

Carrión, C.A., Costa, M.L., Martínez, D.E., Mohr, C., Humbeck, K. and Guiamet, J.J. (2013) *In vivo* inhibition of cysteine proteases provides evidence for the involvement of 'senescence-associated vacuoles' in chloroplast protein degradation during dark-induced senescence of tobacco leaves. *J. Exp. Bot.* **64**, 4967–4980.

Chandrasekar, B., Colby, T., Emon, A.E.K., Jiang, J., Hong, T.N., Villamor, J.G., Harzen, A., Overkleeft, H.S. and van der Hoorn, R.A.L. (2014) Broad range glycosidase activity profiling. *Mol. Cell Proteomics*, **13**, 2787–2800.

Charif, D. and Lobry, J. (2007) SeqinR 1.0–2: a contributed package to the R project for statistical computing devoted to biological sequences retrieval and analysis. In *Structural Approaches to Sequence Evolution* (Bastolla, U., Porto, M., Roman, H.E. and Vendruscolo, M., eds). Berlin: Springer, pp. 207–232.

Chen, P. and Hochstrasser, M. (1996) Autocatalytic subunit processing couples active site formation in the 20S proteasome to completion of assembly. *Cell*, **86**, 961–972.

Cox, J. and Mann, M. (2008) MaxQuant enables high peptide identification rates, individualized p.p.b.-range mass accuracies and proteome-wide protein quantification. *Nat. Biotechnol.* **26**, 1367–1372.

Cox, J., Neuhauser, N., Michalski, A., Scheltema, R.A., Olsen, J.V. and Mann, M. (2011) Andromeda: a peptide search engine integrated into the MaxQuant environment. *J. Proteome Res.* **10**, 1794–1805.

Cox, J., Hein, M.Y., Luber, C.A., Paron, I., Nagaraj, N. and Mann, M. (2014) Accurate proteome-wide label-free quantification by delayed normalization and maximal peptide ratio extraction, termed MaxLFQ. *Mol. Cell Proteomics*, **13**, 2513–2526.

Cravatt, B.F., Wright, A.T. and Kozarich, J.W. (2008) Activity-based protein profiling: from enzyme chemistry to proteomic chemistry. *Annu. Rev. Biochem.* **77**, 383–414.

Dahan, J., Etienne, P., Petitot, A.S., Houot, V., Blein, J.P. and Suty, L. (2001) Cryptogein affects expression of α3f, α6 and β1 proteasome subunits encoding gene in tobacco. *J. Exp. Bot.* **52**, 1947–1948.

Dick, T.P., Nussbaum, A.K., Deeg, M. *et al.* (1998) Contribution of proteasomal β-subunits to the cleavage of peptide substrates analyzed with yeast mutants. *J. Biol. Chem.* **273**, 25637–25646.

Dong, S., Stam, R., Cano, L.M. *et al.* (2014) Effector specialization in a lineage of the Irish potato famine pathogen. *Science*, **343**, 552–555.

Gallois, J.L., Guyon-Debast, A., Le′ cureuil, A., Vezon, D., Carpentier, V., Bonhomme, S. and Guerche, P. (2009) The Arabidopsis proteasome RPT5 subunits are essential for gametophyte development and show accession-dependent redundancy. *Plant Cell*, **21**, 442–459.

Goodin, M.M., Zaitlin, D., Naidu, R.A. and Lommel, S.A. (2008) *Nicotiana benthamiana*: its history and future as a model for plant–pathogen interactions. *Mol. Plant Microbe Interact.* **21**, 1015–1026.

Greenbaum, D., Medzihradszky, K.F., Burlingame, A. and Bogyo, M. (2000) Epoxide electrophiles as activity-dependent cysteine protease profiling and discovery tools. *Chem. Biol.* **7**, 569–581.

Groll, M., Ditzel, L., Löwe, J., Stock, D., Bochtler, M., Bartunik, H.D. and Huber, R. (1997) Structure of 20S proteasome from yeast at 2.4 A resolution. *Nature*, **386**, 463–471.

Groll, M., Schellenberg, B., Bachmann, A.S., Archer, C.R., Huber, R., Powell, T.K., Lindow, S., Kaiser, M. and Dudler, R. (2008) A plant pathogen virulence factor inhibits the eukaryotic proteasome by a novel mechanism. *Nature*, **452**, 755–758.

Gu, C. (2009) *Activity-based protein profiling in plants*. PhD Thesis, University of Cologne.

Gu, C., Kolodziejek, I., Misas-Villamil, J.C., Shindo, T., Colby, T., Verdoes, M., Richau, K.H., Schmidt, J., Overkleeft, H.S. and van der Hoorn, R.A.L. (2010) Proteasome activity profiling: a simple, robust and versatile method revealing subunit-selective inhibitors and cytoplasmic, defence-induced proteasome activities. *Plant J.* **62**, 160–170.

van der Hoorn, R.A.L., Leeuwenburgh, M.A., Bogyo, M., Joosten, M.H.A.J. and Peck, S.C. (2004) Activity profiling of papain-like cysteine proteases in plants. *Plant Physiol.* **135**, 1170–1178.

Hörger, A.C., Ilyas, M., Stephan, W., Tellier, A., van der Hoorn, R.A.L. and Rose, L.E. (2012) Balancing selection at the tomato RCR3 guardee gene family maintains variation in strength of pathogen defense. *PLoS Genet.* **8**, e1002813.

Kaschani, F., Shabab, M., Bozkurt, T., Shindo, T., Schornack, S., Gu, C., Ilyas, M., Win, J., Kamoun, S. and van der Hoorn, R.A.L. (2010) An effector-targeted protease contributes to defense against *Phytophthora infestans* and is under diversifying selection in natural hosts. *Plant Physiol.* **154**, 1794–1804.

Kisselev, A.F., Kopian, T.N., Castillo, V. and Goldberg, A.L. (1999) Proteasome active sites allosterically regulate each other, suggesting a cyclical bite-chew mechanism for protein breakdown. *Mol. Cell*, **4**, 395–402.

Kolodziejek, I., Misas-Villamil, J.C., Kaschani, F. *et al.* (2011) Proteasome activity imaging and profiling characterizes bacterial effector Syringolin A. *Plant Physiol.* **155**, 477–489.

Kurepa, J. and Smalle, J.A. (2008a) Structure, function and regulation of plant proteasomes. *Biochimie*, **90**, 324–335.

Larkin, M.A., Blackshields, G., Brown, N.P. *et al.* (2007) Clustal W and Clustal X version 2.0. *Bioinformatics*, **23**, 2947–2948.

Lee, K.H., Minami, A., Marshall, R.S., Book, A.J., Farmer, L.M., Walker, J.M. and Vierstra, R.D. (2011) The RPT2 subunit of the 26S proteasome directs complex assembly, histone dynamics, and gametophyte and sporophyte development in Arabidopsis. *Plant Cell*, **23**, 4298–4317.

Li, N., Kuo, C.L., Paniagua, G. *et al.* (2013) Relative quantification of proteasome activity by activity-based protein profiling and LC-MS/MS. *Nat. Protoc.* **8**, 1155–1168.

Livak, K.J. and Schmittgen, T.D. (2001) Analysis of relative gene expression data using real-time quantitative PCR and the 2(-Delta Delta C(T)) Method. *Methods*, **25**, 402–408.

Lozano-Torres, J.L., Wilbers, R.H.P., Gawronski, P., et al. (2012) Dual disease resistance mediated by immune receptor Cf-2 in tomato require a common virulence target of a fungus and a nematode. *Proc. Nat. Acad. Sci. USA*, **109**, 10119–10124.

Martínez, D.E., Bartoli, C.G., Grbic, V. and Guiamet, J.J. (2007) Vacuolar cysteine proteases of wheat (*Triticum aestivum* L.) are common to leaf senescence induced by different factors. *J. Exp. Bot.* **58**, 1099–1107.

Michalski, A., Damoc, E., Lange, O. *et al.* (2012) Ultra high resolution linear ion trap Orbitrap mass spectrometer (Orbitrap Elite) facilitates top down LC MS/MS and versatile peptide fragmentation modes. *Mol. Cell Proteomics*, **11**, O111.013698. doi: 10.1074/mcp.O111.013698.

Misas-Villamil, J.C., Kolodziejek, I., Crabill, E., Kaschani, F., Niessen, S., Shindo, T., Kaiser, M., Alfano, J.R. and van der Hoorn, R.A.L. (2013) *Pseudomonas syringae* pv. *syringae* uses proteasome inhibitor Syringolin A to colonize from wound infection sites. *PLoS Pathog.* **9**, e1003281.

Morimoto, K. and van der Hoorn, R.A.L. (2016) The increasing impact of activity-based protein profiling in plant science. *Plant Cell Physiol.* **57**, 446–461.

Mueller, A.N., Ziemann, S., Treitschke, S., Aßmann, D. and Doehlemann, G. (2013) Compatibility in the *Ustilago maydis*-maize interaction requires inhibition of host cysteine proteases by the fungal effector Pit2. *PLoS Pathog.* **9**, e1003177.

Nguyen, H.M., Schippers, J.H., Goni-Ramos, O., Christoph, M.P., Dortay, H., van der Hoorn, R.A.L. and Mueller-Roeber, B. (2013) An upstream regulator of the 26S proteasome modulates organ size in *Arabidopsis thaliana*. *Plant J.* **74**, 25–36.

Olsen, J.V., de Godoy, L.M., Li, G., Macek, B., Mortensen, P., Pesch, R., Makarov, A., Lange, O., Horning, S. and Mann, M. (2005) Parts per million mass accuracy on an Orbitrap mass spectrometer via lock mass injection into a C-trap. *Mol. Cell Proteomics*, **4**, 2010–2021.

Padmanabhan, A., Vuong, S.A. and Hochstrasser, M. (2016) Assembly of an evolutionary conserved alternative proteasome isoform in human cells. *Cell Rep.* **14**, 2962–2974.

Paradis, E., Claude, J. and Strimmer, K. (2004) APE: analyses of phylogenetics and evolution in R language. *Bioinformatics*, **20**, 289–290.

Poret, M., Chandrasekar, B., van der Hoorn, R.A.L. and Avice, J.B. (2016) Characterization of senescence-associated protease activities in the efficient protein remobilization during leaf senescence of winter oilseed rape. *Plant Sci.* **246**, 139–153.

Rooney, H., Van't Klooster, J., Van der Hoorn, R.A.L., Joosten, M.H.A.J., Jones, J.D.G. and De Wit, P.J.G.M. (2005) Cladosporium Avr2 inhibits

tomato Rcr3 protease required for Cf-2-dependent disease resistance. *Science*, **308**, 1783–1789.

Schellenberg, B., Ramel, C. and Dudler, R. (2010) *Pseudomonas syringae* virulence factor Syringolin A counteracts stomatal immunity by proteasome inhibition. *Mol. Plant Microbe Interact.* **23**, 1287–1293.

Seifert, U., Bialy, L.P., Ebstein, F. *et al.* (2010) Immuno-proteasomes preserve protein homeostasis upon interferon-induced oxidative stress. *Cell*, **142**, 613–624.

Shabab, M., Shindo, T., Gu, C., Kaschani, F., Pansuriya, T., Chintha, R., Harzen, A., Colby, T., Kamoun, S. and van der Hoorn, R.A.L. (2008) Fungal effector protein AVR2 targets diversifying defence-related Cys proteases of tomato. *Plant Cell*, **20**, 1169–1183.

Song, J., Win, J., Tian, M., Schornack, S., Kaschani, F., Muhammad, I., van der Hoorn, R.A.L. and Kamoun, S. (2009) Apoplastic effectors secreted by two unrelated eukaryotic plant pathogens target the tomato defense protease Rcr3. *Proc. Natl Acad. Sci. USA*, **106**, 1654–1659.

Suty, L., Lequeu, J., Lancon, A., Etienne, P., Petitot, A.S. and Blein, J.P. (2003) Preferential induction of 20S proteasome subunits during elicitation of plant defense reactions: towards the characterization of plant defense proteasomes. *Int. J. Biochem. Cell Biol.* **35**, 637–650.

Tian, M., Win, J., Song, J., Van der Hoorn, R.A.L., Van der Knaap, E. and Kamoun, S. (2007) A *Phytophthora infestans* cystatin-like protein interacts with and inhibits a tomato papain-like apoplastic protease. *Plant Physiol.* **143**, 364–277.

Üstün, S., Bartetzo, V. and Bornke, F. (2013) The *Xanthomonas campestris* type III effector XopJ targets the host cell proteasome to suppress salicylic-acid mediated plant defence. *PLoS Pathog.* **9**, e1003427.

Üstün, S., Konig, P., Guttman, D.S. and Bornke, F. (2014) HopZ4 from *Pseudomonas syringae*, a member of the HopZ type III effector family from the YopJ superfamily, inhibits the proteasome in plants. *Mol. Plant Microbe Interact.* **27**, 611–623.

Üstün, S., Sheikh, A., Gimenez-Ibanez, S., Jones, A., Ntoukakis, V. and Börnke, F. (2016) The proteasome acts as a hub for plant immunity and is targeted by Pseudomonas type III effectors. *Plant Physiol.* **172**, 1941–1958.

Van Esse, H.P., Van't Klooster, J.W., Bolton, M.D., Yadeta, K.A., Van Baarlen, P., Boeren, S., Vervoort, J., De Wit, P.J.G.M. and Thomma, B.P.H.J. (2008) The *Cladosporium fulvum* virulence protein Avr2 inhibits host proteases required for basal defense. *Plant Cell*, **20**, 1948–1963.

Verdoes, M., Willems, L.I., van der Linden, W.A., Duivenvoorden, B.A., van der Marel, G.A., Florea, B.I., Kisselev, A.F. and Overkleeft, H.S. (2010) A panel of subunit-selective activity-based proteasome probes. *Org. Biomol. Chem.* **8**, 2719–2727.

Wang, S., Kurepa, J. and Smalle, J.A. (2009) The Arabidopsis 26S proteasome subunit RPN1a is required for optimal plant growth and stress responses. *Plant Cell Physiol.* **50**, 1721–1725.

Wei, C.F., Kvitko, B.H., Shimizu, R., Crabill, E., Alfano, J.R., Lin, N.C., Martin, G.B., Huang, H.C. and Collmer, A. (2007) A *Pseudomonas syringae* pv. *tomato* DC3000 mutant lacking the type III effector HopQ1-1 is able to cause disease in the model plant *Nicotiana benthamiana*. *Plant J.* **51**, 32–46.

Wessel, D. and Flügge, U.I. (1984) A method for the quantitative recovery of protein in dilute-solution in the presence of detergents and lipids. *Anal. Biochem.* **138**, 141–143.

Yang, P., Fu, H., Walker, J.M., Papa, C.M., Smalle, J.A., Ju, Y.M. and Vierstra, R.D. (2004) Purification of the Arabidopsis 26S proteasome: biochemical and molecular analyses revealed the presence of multiple isoforms. *J. Biol. Chem.* **279**, 6401–6413.